Science of the Total Environment 787 (2021) 147701

Contents lists available at ScienceDirect

Science of the Total Environment

journal homepage: www.elsevier.com/locate/scitotenv

Influence of land-use change and season on soil greenhouse gas emissions from a tropical wetland: A stepwise explorative assessment

Risper Ajwang' Ondiek [a,*,1], Daniel S. Hayes [a,b,1], Damaris Njeri Kinyua [a], Nzula Kitaka [c], Erwin Lautsch [a], Paul Mutuo [d], Thomas Hein [a,e]

[a] Institute of Hydrobiology and Aquatic Ecosystem Management, University of Natural Resources and Life Sciences, Gregor Mendel Straße 33, 1180 Vienna, Austria
[b] Forest Research Center, Instituto Superior de Agronomia, University of Lisbon, Tapada da Ajuda, 1349-017 Lisbon, Portugal
[c] Department of Biological Sciences, Egerton University, P.O. Box 536, Nakuru 20115, Kenya
[d] Mazingira Centre, International Livestock Research Institute (ILRI), P.O. Box 30709, Nairobi 00100, Kenya
[e] WasserClusterLunz — Biologische Station GmbH, Dr. Carl Kupelwieser Promenade 5, 3293 Lunz am See, Austria

HIGHLIGHTS

- CO_2 emissions are influenced by season and not land-use change.
- Conversion of wetlands to farmland promotes CH_4 uptake regardless of the season.
- Conversion of wetlands to farmland increases N_2O emissions during the dry season.
- Beyond season and land-use, analyses reveal the effects of soil parameters on emissions.
- Wetland conversion to farmland jeopardizes climate change mitigation.

GRAPHICAL ABSTRACT

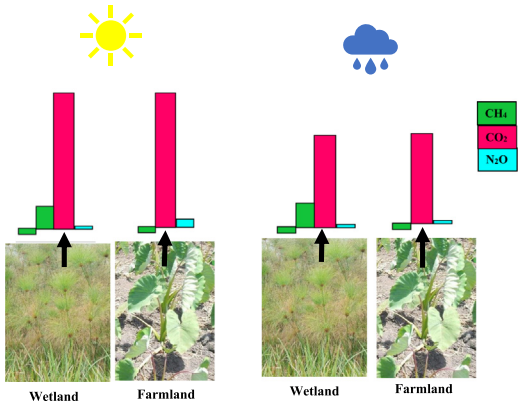

ARTICLE INFO

Article history:
Received 5 March 2021
Received in revised form 6 May 2021
Accepted 7 May 2021
Available online 13 May 2021

Editor: Fernando A.L. Pacheco

Keywords:
East Africa
Afrotropical region
Papyrus
Heuristic methods
Classification and regression tree (CRT)
Configuration frequency analysis

ABSTRACT

Tropical wetlands are important climate regulators. However, their climate regulating function is at risk by land-use conversion for agricultural purposes. In sub-Saharan Africa, studies investigating the effect of land-use change in wetlands and associated soil greenhouse gas (GHG) emissions remain limited. Moreover, the influence of season in GHG emissions with land-use change has hardly been studied. Therefore, we investigated methane (CH_4), carbon dioxide (CO_2), and nitrous oxide (N_2O) emissions from a Kenyan wetland and adjacent areas converted to farmland during the dry and rainy seasons. Moreover, we assessed which soil parameters drive the variations in GHG emissions. The GHG samples were collected by the static chamber method and analyzed by gas chromatography. For data analysis, we employed an explorative-statistical approach to explain the emission rates' variation and determine which parameters influence the GHG emissions, both as main and interaction effects. The results showed that regardless of the season, there were CH_4 emissions (>0.50 mg m^{-2} h^{-1}) from the wetland when soil organic carbon content was high and uptake (<0.001 mg m^{-2} h^{-1}) when both soil organic carbon content and soil moisture were low. In the farmland, there was CH_4 uptake when soil nitrate-nitrogen content was high. CO_2 emissions did not vary significantly between the land-use types. Instead, emission rates were primarily governed by season. The highest emissions (>175 mg m^{-2} h^{-1}) during the dry season were attributed to high soil organic carbon content. During the rainy season, emissions hardly exceeded 175 mg m^{-2} h^{-1}. Regarding N_2O, we detected the highest emissions (>5 μg m^{-2} h^{-1}) from the farmland during the dry

* Corresponding author.
E-mail address: ondiek.risper7@gmail.com (R.A.' Ondiek).
[1] Equally contribution authors.

https://doi.org/10.1016/j.scitotenv.2021.147701

season. Overall, this study shows that wetland conversion to farmland encourages CH_4 uptake regardless of the season and increases N_2O emissions during the dry season. Based on the respective GHG global warming potential, these patterns may pose an increased environmental threat.

1. Introduction

Wetlands cover around 5–8% of the earth's surface area (7–10 million km^2) but constitute one of the largest natural sources of greenhouse gases (GHGs) (Mitsch and Gosselink, 2007). According to Mitsch et al. (2013), even though wetlands emit CH_4, they constitute net carbon sinks of about 830 Tg-C $year^{-1}$. For example, wetlands sequester about 1280 Tg-C $year^{-1}$ of CO_2 from the atmosphere and emit 448 Tg-C $year^{-1}$ of CH_4 back into the atmosphere (Mitsch et al., 2013). Therefore, wetlands are essential climate regulators, underlining the urgency of promoting their sustainable use (Batson et al., 2015; Liu et al., 2017; Zedler and Kercher, 2005).

Wetlands are among the most threatened ecosystems worldwide (Houghton et al., 2012; MEA, 2005). Their decline is mainly attributed to conversion to agriculture due to increasing food demand (MEA, 2005). Also, increased river water withdrawals due to economic development contribute to the wetland decline (Dixon and Wood, 2003; Hayes et al., 2018; Junk et al., 2013; Mitchell, 2013). During the twentieth century alone, over 50% of all wetland areas in Europe, North America, New Zealand, and Australia were converted to agriculture (MEA, 2005). For other regions, the quantities remain speculative as reliable data are missing (MEA, 2005). In Kenya, for instance, studies estimate that the losses range between 34 and 55% during the last four to five decades. In these cases, the conversion to agriculture is the primary reason for this decline (Ondiek et al., 2020; Owino and Ryan, 2007). Although the conversion and drainage of wetlands contribute to crop production, soil GHG emissions from the ecosystem may also be altered, putting the climate regulating function of wetlands at stake (Nath and Lal, 2017; Zedler and Kercher, 2005).

Land-use change can alter the emissions of soil GHG such as CO_2, N_2O, and CH_4. The drainage of peatlands to agricultural land, for example, can lead to enhanced emissions of N_2O and CO_2 while simultaneously decreasing CH_4 emissions (Smith and Conen, 2004). Alteration of wetland's hydrology through drainage and cultivation interferes with the ecosystems' anaerobic conditions. Under aerobic conditions, soil organic matter decomposes much faster, increasing CO_2 emissions (Mitsch et al., 2013; Smith and Conen, 2004). In contrast, flooding inhibits the atmospheric oxygen supply to the soil, resulting in anaerobic decomposition of soil organic matter (Reddy and DeLaune, 2008), leading to increased CH_4 production. Methane is a potent GHG that, over a 100-year period, has a 25-fold global warming potential than that of CO_2 (Whiting and Chanton, 2001). Therefore, the drainage of wetlands can contribute to mitigating CH_4 emissions, as they produce 20–25% of global CH_4 emissions (ca. 115–227 Tg $year^{-1}$) (Bergamaschi et al., 2007; Bloom et al., 2010; Whalen, 2005). Of these emissions, tropical wetlands emit a substantial share of around 138 Tg $year^{-1}$ (Bergamaschi et al., 2007).

Nitrous oxide is another potent GHG. It has a global warming potential 300 times that of CO_2 over a 100-year period (IPCC, 2013). Nitrous oxide emissions from wetlands stem from coupled nitrification-denitrification processes (Bernal and Mitsch, 2012; Hernandez and Mitsch, 2007). However, under strictly anaerobic conditions in wetlands, the major end-product of denitrification is N_2, thus reducing N_2O emissions (Butterbach-Bahl et al., 2013; Reddy and DeLaune, 2008). However, the drainage and conversion of wetlands to intensified agriculture are known to increase N_2O emissions because of increased nitrogen input from fertilizer application and aerobic soil conditions (Reddy and DeLaune, 2008). In sub-Saharan Africa (SSA), however, smallholder farms, which encompass nearly 80% of farmland and up to 90% of farms, apply only a little or no fertilizer at all (Altieri and Koohafkan, 2008; Pelster et al., 2017). Therefore, under such non-intensive agricultural practices, it remains to be elucidated if the conversion of wetlands to agriculture enhances N_2O emissions.

Given the importance of wetlands in biogeochemical cycles, their conversion to agriculture is expected to have considerable impacts on national and regional GHG emission budgets. The changes in GHG emissions with land-use change are also expected to be influenced by the seasonal changes related to dry and rainy periods. However, knowledge on the biogeochemistry of tropical wetlands remains limited (Bernal and Mitsch, 2013), as most relevant studies were conducted in temperate regions with entirely different climatic conditions than those in the tropics (Bridgham et al., 2006; Euliss et al., 2006; Tangen et al., 2015). Few studies assessed the effect of land-use change on wetland GHG emissions in Africa's tropical region (CO_2: Saunders et al. (2012); N_2O: Tshering (2012)), and, to our knowledge, no research has so far considered seasonal changes. Hence, it is crucial to quantify GHG emissions in different seasons.

Soil properties are the main drivers of soil GHGs production and consumption (Butterbach-Bahl et al., 2013; Davidson and Janssens, 2006). Soil properties such as moisture content control oxygen concentration in soils and subsequently microbial processes such as the degradation of organic matter, thus regulating GHG emissions (Butterbach-Bahl et al., 2013; Reddy and DeLaune, 2008). The production of N_2O, for example, depends on soil conditions, including moisture, pH, temperature, oxygen concentration, carbon, ammonium (NH_4-N), or nitrate (NO_3-N) (Reddy and DeLaune, 2008; Zhu et al., 2013). Therefore, considering that land-use change, and season can modify soil properties, it is expected that the interrelations of these influences determine soil GHG emissions.

This study aims to assess the effects of land-use change, season, and soil properties on soil GHG emissions from wetlands in Africa's tropical region. Therefore, we conducted field measurements of the emission rates of three prevalent GHGs – CH_4, CO_2, and N_2O – from areas converted to farmland and unconverted areas of the Anyiko wetland in Kenya. Our key research question is how season influences the variation in GHGs emissions between the converted and unconverted wetland areas. Also, we aim to identify which soil parameters influence GHGs emissions' variation. The available dataset does not meet the necessary mathematical-statistical preconditions for general linear models (e.g., multivariate distribution properties, number, structure, and selection of cases) and does not meet inferential statistical requirements. This status raises the question of which methodological approach can deal with these preconditions commonly encountered in field studies.

2. Materials and methods

2.1. Study area

The study was conducted in the Anyiko wetland in Siaya County in Kenya (Fig. 1). The wetland is in the Nzoia River Basin, the largest Kenyan sub-basin of Lake Victoria (MEMR, 2012). The Anyiko wetland currently (2018) covers an area of ca. 0.7 km^2 (Ondiek et al., 2020). Papyrus (*Cyperus papyrus* L.) is the dominant vegetation type in the wetland.

The Anyiko wetland receives two rainy seasons (March–May and October–December) annually. The mean annual rainfall is 1556 and

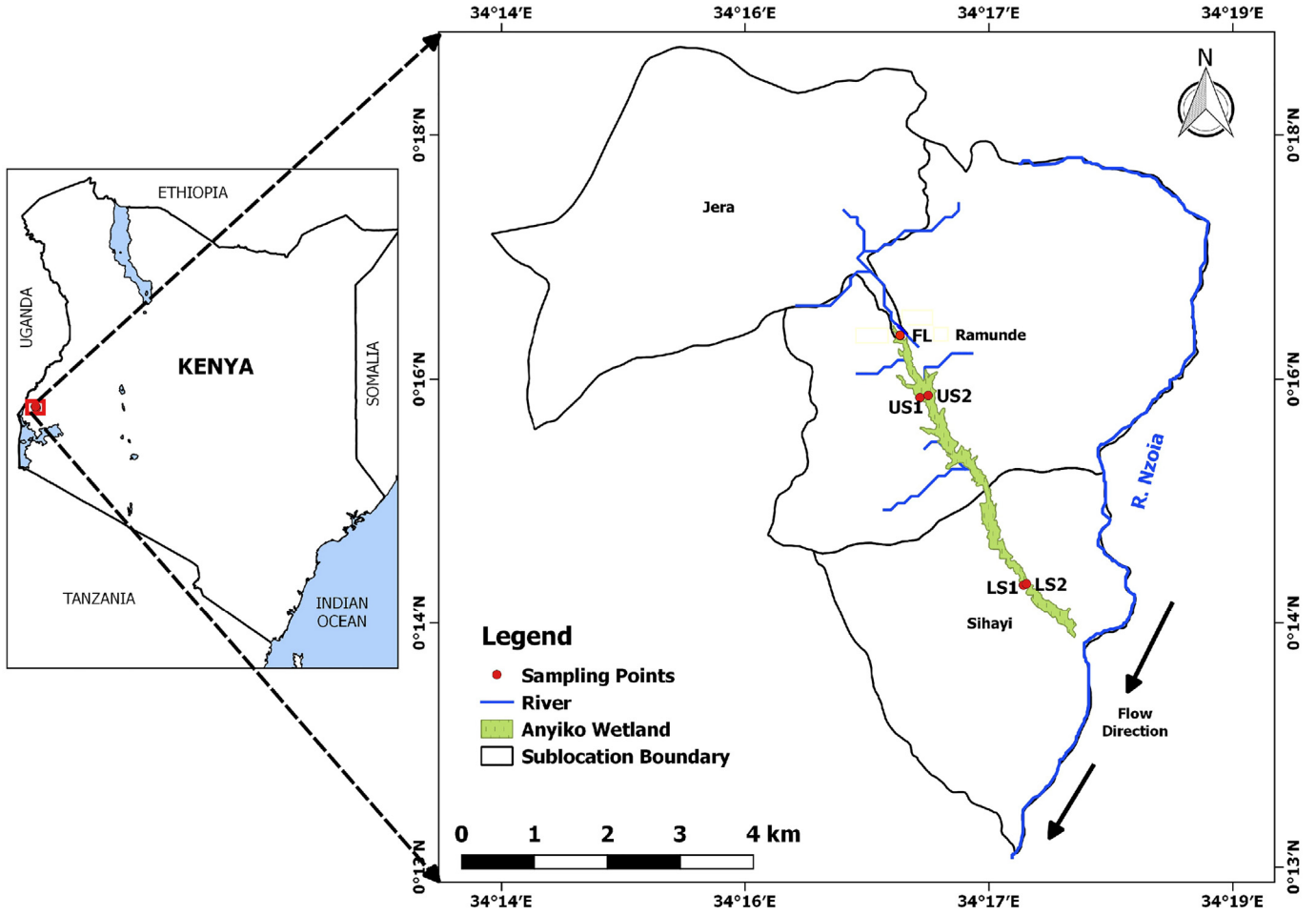

Fig. 1. Location of the Anyiko wetland, Kenya, and sampling sites in the converted and unconverted wetland areas. Four sampling sites are situated in the wetland area (US = upper site, LS = lower site), and one in the areas converted to farmland (FL).

ranges from 813 to 2417 mm between years. The mean annual temperature is 22 °C (range: 16–30 °C). The driest months are January and February with mean temperature of 23 °C and rainfall of 68 mm (County Government of Siaya, 2018).

The Anyiko wetland size has been reduced by 55% (0.9 km^2) in the last five decades (1966–2018) (Ondiek et al., 2020). The main reasons for this trend are wetland drainage and conversion to farmland (−0.7 km^2) but also shrubland encroachment (Ondiek et al., 2020). The local community uses the converted wetland areas primarily for small-scale paddy rice production and the cultivation of cocoyam, maize, and vegetables. Paddy rice is predominantly grown at downstream areas where more water is available for irrigation; cocoyam (*Colocasia esculenta*), maize (*Zea mays*), and vegetables, e.g., collard greens (*Brassica oleracea*) and African nightshade (*Solanum scabrum*), are mostly grown at the upstream areas. Maize is flood-intolerant but is grown during the rainy seasons in relatively well-drained soils. Paddy rice is grown once a year because of inadequate water supply during the 'short' rains. Cocoyam is grown throughout the year and vegetables during the dry season. Therefore, in the downstream areas of the wetland, the converted areas are uncultivated during the dry season. At the upstream areas, the cultivation is more diverse depending on the crop.

2.2. Study design and sampling sites characteristics

We measured soil CH_4, CO_2, and N_2O emissions up to four times a month from 27 December 2017 to 27 May 2018 (total number of sampling dates, $n = 14$). We selected four sampling sites in the wetland (two upstream and two downstream situated sites) and one site in the area converted to cocoyam farming (Fig. 1). The four sampling sites in the wetland included: Upper site 1 (US1), Upper site 2 (US2), Lower site 1 (LS1), and Lower site 2 (LS2) (Fig. 1). During the rainy season, only two wetland sites — upper site 2 (US2) and lower site 1 (LS1), were sampled.

2.3. Soil GHG sampling

We measured soil CO_2, CH_4, and N_2O emissions with the closed static chamber technique (Pumpanen et al., 2004), according to the minimum requirements for GHG (Butterbach-Bahl et al., 2016; Parkin and Venterea, 2010). The chamber technique is commonly used to measure soil GHG fluxes because it is relatively inexpensive, simple to operate, and flexible (Butterbach-Bahl et al., 2011). However, the technique underestimates GHG fluxes due to an altered diffusion gradient slowing the gas diffusion from the soil after putting the chamber on the soil surface (Pumpanen et al., 2004).

We fabricated the chambers from ten-liter opaque plastic buckets comprising of two parts: a base (25 cm diameter and 15 cm height) and a lid (25 cm diameter and 25 cm height). The lid was fitted with a gas sampling port, a vent tube (50 cm long and 2.5 mm diameter), and a thermometer (Pelster et al., 2017; Tully et al., 2017). In order to minimize temperature increases inside the chambers (Butterbach-Bahl et al., 2011), we insulated them with reflective tape.

We installed the chamber bases at the sampling sites two weeks before the first GHG measurement. In the unconverted areas, we had to clear above-ground papyrus biomass to provide room for installing the chamber bases. Each sampling site consisted of three randomly

selected clusters as replicates for the GHG measurements. We inserted three chamber bases 7–10 cm into the soil at each cluster, totaling nine chamber bases per site. During the rainy season, the chamber bases at US2 were removed and adjusted to 35–40 cm height due to increased water level and re-inserted into the soil. The chamber bases were also equipped with 2–4 holes to ensure water flow between the chamber and its surrounding (Butterbach-Bahl et al., 2016). The overlying water in the chambers enhances anaerobic conditions in the soil, allowing the growth of methanogens that use carbon compounds as electron donors and producing CH_4 in anaerobic respiration (Butterbach-Bahl et al., 2016). Hence, CH_4 emissions may be higher in the chamber than in the surrounding area if there are no holes in the chamber bases. The holes above the water layer were closed before sampling when the water level dropped in the chambers. Closing of the holes eliminates air diffusion from inside to outside of the chambers, thereby averting underestimation of GHG emissions. Towards the end of the dry season, farmers dug a canal along LS1 to prevent flooding into the adjacent rice paddies during the rainy season. Water flowing along LS1 was, therefore, mostly restricted to the canal.

The chamber bases remained in place throughout the sampling period to minimize soil disturbance. Occasionally, some got damaged or went missing due to livestock trampling, wetland burning, or vandalization. However, these were quickly replaced (at least one week before the next gas sampling). Chamber bases were also removed during cocoyam farm weeding and re-inserted after soil management. During the rainy season, boardwalks built at each sampling site minimized CH_4 emissions due to sediment disturbance/vibrations (Butterbach-Bahl et al., 2016). We conducted gas sampling between 10:00 am and 1:00 pm and between 4:00 pm and 6:00 pm, thereby covering the diurnal cycle's average flux (Minamikawa et al., 2012; Parkin and Venterea, 2010).

At each sampling event, we cut growing shoots of papyrus in the chambers to ground level before sampling. We ensured the chamber's airtightness by using rubber seals to clamp the bases and lids together (Rochette, 2011). We closed the chambers for 30 min and collected air samples (60 ml) inside the chambers from the headspace every 10 min (0, 10, 20, and 30 min) using polypropylene syringes (60 ml capacity) fitted with Luer locks. Using the gas-pooling technique, we ensured that the soil's spatial heterogeneity in the two land-use types is appropriately depicted (Arias-Navarro et al., 2013). At each of the above-mentioned intervals, we collected 20 ml of headspace air from each of the three chambers. We used the first 40 ml of each 60 ml composite gas sample to flush the vials. We then filled the remaining 20 ml into 10 ml glass vials. This stepwise approach guarantees that gas contamination with ambient air is minimized (Rochette and Bertrand, 2003). Also, at each time interval before gas collection, we manually mixed air inside the chamber by drawing and pumping the air back and forth severally. The gas samples were transported to the Mazingira Centre, International Livestock Research Institute (ILRI) for analysis.

2.4. Soil GHG analysis

The gas samples were analyzed for CO_2, CH_4, and N_2O using gas chromatography (SRI 8610C gas chromatograph). We calculated the GHG concentrations from the sample's peak areas relative to the four regular calibration gases' peak areas. We converted the gas concentrations to mass per volume flux according to Butterbach-Bahl et al. (2011). We computed the chamber fluxes if $R^2 \geq 0.70$ (Rochette and Bertrand, 2008). Also, we examined the CO_2 concentration dynamics over the 30 min period to validate the data for each chamber measurement. Chambers with a CO_2 decrease >10% between any time intervals were assumed to leak. In such a case, we discarded all gas fluxes from further analysis. The only exception was when the decrease occurred in the last measurement, as we could still calculate the flux rate with the first three measurement points (Pelster et al., 2017). However, if there was no leakage, negative CH_4 and N_2O values were recognized as the soil's uptake of the respective GHG. The minimum detection limits for each gas were $\pm$ 0.02 mg CH_4-C m^{-2} h^{-1}, $\pm$3.1 mg CO_2-C m^{-2} h^{-1}, and $\pm$3.5 μg N_2O-N m^{-2} h^{-1}. However, we included all the data, even those below the minimum detection limit in the analysis as recommended by Croghan and Egeghy (2003) and Parkin et al. (2012).

2.5. Measurements of soil parameters

At each gas-sampling event, we measured soil temperature at a depth of 0–20 cm next to the chamber bases with a digital thermometer (Brannan 31/162/0). Also, we collected one soil sample (depth: 0–15 cm) from each of the three randomly selected clusters per sampling site. We then determined soil moisture by oven-drying a weighed amount of the samples for 48 h at 105 °C and re-weighing them after cooling. We calculated the soil moisture on a dry weight basis (Okalebo et al., 2002). The remaining soil samples were analyzed for organic carbon, total phosphorus, total nitrogen, ammonium-nitrogen, and nitrate-nitrogen. We determined total nitrogen by the Kjeldahl method, total phosphorus by the ascorbic acid method, organic carbon by the Walkley-Black method, and ammonium-nitrogen and nitrate-nitrogen by the colorimetric method (Okalebo et al., 2002). See Table 1 for an overview of all parameters.

2.6. Data analyses

The general linear model (GLM) presents itself as a suitable approach to answer our research questions. However, the dataset violated the minimum requirements or conditions for the GLM, such as multi-

Table 1
Overview of parameters.

Code	Short name	Description	Unit	Effect status
Y_1	CH_4_Emissions	Methane emissions	mg m^{-2} h^{-1}	–
Y_2	CO_2_Emissions	Carbon dioxide emissions	mg m^{-2} h^{-1}	–
Y_3	N_2O_Emissions	Nitrous oxide emissions	μg m^{-2} h^{-1}	–
X_1	S_Mst	Soil moisture	%	Direct (independent)
X_2	S_Temp	Soil temperature	°C	Direct (independent)
X_3	OC	Organic carbon	%	Direct (independent)
X_4	TN	Total nitrogen	%	direct (independent)
X_5	CN_R	Carbon: nitrogen ratio		Direct (independent)
X_6	TP	Total phosphorus	ppm	Direct (independent)
X_7	CP_R	Carbon: phosphorus ratio		Direct (independent)
X_8	NO_3_N	Nitrate nitrogen	g kg^{-1}	Direct (independent)
$X_{M=9}$	NH_4_N	Ammonium nitrogen	g kg^{-1}	Direct (independent)
X_1'	Season		Nominal: 1 = dry season, 2 = rainy season	Indirect (solitarily)
X_2'	Land-use		Nominal: 1 = wetland, 2 = farmland	Indirect (solitarily)
Z_1	Profile variable	X_1' & X_2' {season & land-use}	Nominal: 1 = [dry season & wetland], 2 = [dry season & farmland], 3 = [rainy season & wetland], 4 = [rainy season & farmland]	Indirect (connected)

dimensional normal distribution and variance homogeneity. Also, the data collection and the targeted arbitrary site selection prohibited strictly inferential statistical data analysis approaches. For such cases, however, the literature offers hypothesis-generating evaluation strategies (e.g., Tukey, 1977). Here, as an alternative to the GLM, we offer a step sequence that has decision tree analysis at its center.

Considering that the metric requirements were not given (Wall and Lienert, 1976; Lienert, 1978), we transformed each of the three continuously-scaled dependent variables (Y_i) into ordinally-scaled variables to allow the prediction of interaction ranges (Table 2). Testing these classified (trichotomized) variables with a log-linear model (LLM) for contingency supported the assumption of total independence of the three GHGs. Moreover, of the eleven independent variables, season (X_1') and land use (X_2') had the status of a controlling (indirect) effect (Table 1). Hence, we merged both controlling effects into one profile variable (Z_1). Formally, the three univariate, multi-factorial models could therefore be expressed as:

$$\left\{ \begin{bmatrix} Y_1 \\ Y_2 \\ Y_3 \end{bmatrix} \leftarrow X_1, X_2, X_3, \ldots, X_8, X_9 \right\} Z_1; \text{for j} = 1(1)3; \text{m} = 1(1)9 \text{ and } Z_1 = [X'_{1i} \& X'_{2i}] \quad (1)$$

For data analysis, we used the following step sequence.

In the first step, we identified relevant parameters (main and interaction effects) through decision tree analysis (classification and regression tree/CRT; Breiman et al. (1984). The decision tree method corresponds to a graphical, non-linear, scale-independent, stepwise regression/discriminant analysis. We ran a decision tree (SPSS-module: TREE/CRT) for each of the GHGs as the dependent variable (see formula 1). The variable Z_1 {season & land-use} received the highlighted status of a controlling (indirect) effect. Therefore, Z_1 was placed at the first split in all CRT models. The decision which parameters have influence was determined by the Gini-coefficient, a splitting criterion that constitutes an internal measure of homogeneity (IBM Statistics, 2016). Subsequently, we assessed the overall strength of the model fit (model accuracy) through a classification table showing the number of correctly and incorrectly classified cases for each category of the dependent variable (observed versus predicted) (IBM Statistics, 2016).

In the second step, we conducted an exploratory evaluation of the identified effects, particularly the interaction effects, by using a local cross-classification analysis (configuration frequency analysis/CFA; Von Eye, 2002; Von Eye et al., 2010). With this analysis, we examined which of the trees' end nodes contribute to model explanation (node versus categories of the respective GHG), thereby possibly indicating a statistical trend. We determined global significance through chi-square tests. Cramér's V served as an effect size measurement. Local significance was evaluated through Bonferroni-adjusted cell-residual tests to correct for alpha-inflation. Thereby, we could check which single cells affect the target variable. In this regard, it should be noted that, although inferential statistical methods are used in the second step, the reader must not interpret the results strictly. Instead, they serve as an orientation aid for the explorative interpretation (formulation of trend statements).

Although the data quality had not been checked concerning essential statistical quality criteria of a sample (i.e., *validity*, *reliability*, *objectivity*), this working step sequence allowed us to generate hypotheses and describe to what extent there is a possibility that the results are stable.

Table 2
Class boundaries of the ordinally-scaled target variables for the exploratory analyses.

GHGs	Classified: group boundaries		Frequency
CH_4	1	<0.001	20
	2	0.001–0.49	17
	3	≥0.5	32
CO_2	1	<50.0	11
	2	50.0–174.99	26
	3	≥175.0	32
N_2O	1	<5.0	25
	2	5.0–19.99	25
	3	≥20.0	19

Note: Groups were delimited to achieve an approximately equal distribution of cases, and scientifically post-classified. For CH_4, the values <0.001 are negative, thus showing uptake.

3. Results

This study aims to clarify the emission intensity of three prevalent greenhouse gases – CH_4, CO_2, N_2O – depending on two land-use types, two seasons, and nine soil parameters (Table 1). The non-fulfillment of inferential statistical requirements forced us to carry out a stepwise exploratory (hypothesis-generating) analysis approach for each of the three GHGs. The analysis approach comprised of decision tree analyses to determine main and interaction effects, followed by cross-classification analyses for the exploratory evaluation of identified effects. In the next sections, we report the results for each of the three GHGs.

3.1. CH_4 emissions

The CRT method's graphical output is a tree that is split according to selected environmental variables. In addition to revealing which features explain the variation of the target variable, the tree also shows interactions between selected parameters. These interaction effects become visible when one follows a given node sequence, starting from node 0 and moving downwards at each split until an end node is reached. The number of nodes in an interaction sequence reveals a one- (one node), two- (two nodes), or more-fold effect.

The base sample's CH_4 emission tree of selected four different variables (season & land-use, nitrate-nitrogen, organic carbon, and soil moisture). The values <0.001 mg m^{-2} h^{-1} were negatives, indicating CH_4 uptake. Also, as shown by Fig. 3, five effects were essential in assessing the variation of CH_4 emissions in the study area. All five effects were characterized by two- to three-fold interactions, read as interaction paths via the tree nodes. The first interaction effect pathway (IP1: node 0 ⇒ node 1 ⇒ end node 3) indicated that regardless of the season, but only in the farmland, medium emissions were supported by NO_3-N ≤ 0.04 g kg^{-1}. The second pathway (IP2: node 0 ⇒ node 1 ⇒ end node 4) shared the land-use type with the first but then signaled that NO_3-N > 0.04 g kg^{-1} supported CH_4 uptake. On the contrary, the third interaction effect pathway (IP3: node 0 ⇒ node 2 ⇒ end node 6) suggested that in the wetland and irrespective of the season, high emissions were supported by organic carbon content >2.7%. The fourth interaction chain (IP4: node 0 ⇒ node 2 ⇒ node 5 ⇒ end node 7) showcased that in the wetland, CH_4 uptake was connected to organic carbon ≤2.7% and soil moisture <90%. As signaled by the fifth pathway (IP5: node 0 ⇒ node 2 ⇒ node 5 ⇒ end node 8), soil moisture >90% supported the medium emissions (Fig. 2).

Overall, the four selected variables could sufficiently illustrate the variations in CH_4 emissions, as three-quarters of all cases were correctly predicted. In detail, the high emissions group performed best. The uptake and medium emissions groups showed a slightly lower probability for correct classification (Table 3).

After identifying the interaction pathways, we assessed which effects are most probable and may be generalized from a hypothesis-generating perspective. Therefore, we conducted cross-classification analyses with cell-wise post hoc tests. In this regard, the residuals (z) that become apparent in the analysis aid in trend interpretation if they exceed the significance threshold. The higher the residual value, the higher the probability that the results are generalizable.

As shown in Table 4, seven of 15 cells of the CH_4 tree were statistically significant. All interaction pathways except IP1 demonstrated a significant trend in one to three cells. Considering that the residual of

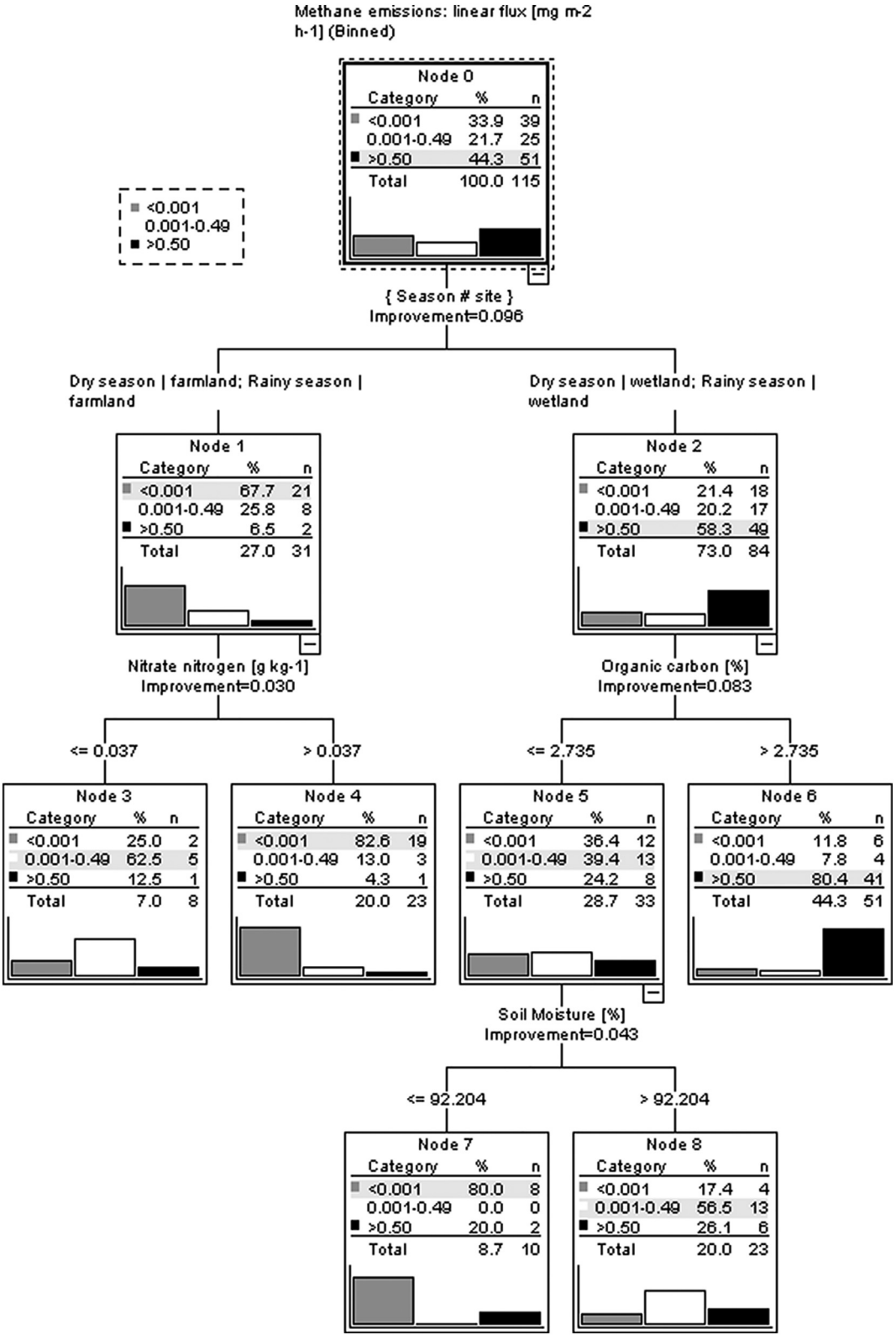

Fig. 2. Explorative decision tree (CRT) of the effects of land-use & season and soil parameters on CH_4 emissions. Minimum numbers of cases per parent node: 12; per child node: 8.

the low emission group of IP5 was only slightly above the significance threshold, it must be treated with care. In contrast, the high residual values of the other pathways suggested a high hit probability, particularly those of IP2 and IP3. The second pathway revealed that at soil NO_3-N > 0.04 g kg^{-1}, there was a likelihood of CH_4 uptake in farmland. On the contrary, as shown by IP3, CH_4 emissions from the wetland were likely if soil organic carbon exceeded 2.7%. However, at lower soil organic carbon content and lower soil moisture ≤90%, there was CH_4 uptake in the wetland (IP4); if soil moisture exceeded 90%, emissions occurred (IP5).

Table 3
Classification table (observed versus predicted) of the CH_4 emissions tree (see Fig. 2).

Observed	Predicted			Percent correct
	1: <0.001	2: 0.001–0.49	3: ≥0.50	
1: <0.001	27	6	6	69.2%
2: 0.001–0.49	3	18	4	72.0%
3: ≥0.50	3	7	41	80.4%
Overall percentage	28.7%	27.0%	44.3%	74.8%

3.2. CO_2 emissions

The CO_2 base sample tree selected two variables, season & land-use and organic carbon, and identified four effects that explained emissions rates' variation. Each of the effects constituted a two-fold interaction (Fig. 3). The first interaction effect pathway (IP1: node 0 ⇒ node 1 ⇒ end node 3) signaled that during the dry season but irrespective of land-use type, organic carbon ≤2.6% promoted medium CO_2 emissions. The second pathway (IP2: node 0 ⇒ node 1 ⇒ end node 4) shared the dry season effect with the first but then indicated that higher organic carbon content promoted the highest emissions. The third and fourth pathways were both governed by the rainy season, showing mostly low to medium emission rates, but were then split according to land-use: low emissions cases dominated in the third pathway describing the farmland (IP3: node 0 ⇒ node 2 ⇒ end node 5), whereas the fourth pathway describing the wetland (IP4: node 0 ⇒ node 2 ⇒ end node 6) was characterized by a higher share of medium emission cases and an almost entire lack of high emission cases (Fig. 3).

Overall, the four effects correctly predicted 70% of the cases. Similar to the CH_4 tree, the high emissions group performed best, followed by the medium group. Only the low group showed a lower correct classification probability; only one-third of cases were correctly predicted (Table 5).

Preceding with the cell tests, we found that more than half of the cells exceeded the threshold of significance and that each of the four interaction pathways demonstrated a significant trend in at least one of its cells. In particular, the high residual values in IP2–4 suggested a high hit probability. During the dry season, at soil organic carbon content ≤2.6% and >2.6%, CO_2 emissions were more likely to be moderate and high, respectively. However, during the rainy season, the emissions were more likely to be low in the farmland (IP3) and in wetland (IP4). Regarding the latter, emissions were also less likely to be high (Table 6).

Table 4
Cross-classification table (CFA) results for the end nodes (interaction pathways) versus CH_4 emission groups (see Fig. 2).

Interaction pathway (IP) → end node		CH_4 emissions [$mgm^{-2}\ h^{-1}$]: classified			Total
		1: <0.001	2: 0.001–0.49	3: ≥0.50	
IP1: {Node 0 ⇒ 1 ⇒ end node 3}	n	2	5	1	8
	e	2.7	1.7	3.5	8
	z	−0.6	2.9	−1.9	
IP2: {Node 0 ⇒ 1 ⇒ end node 4}	n	19	3	1	23
	e	7.8	5.0	10.2	23
	z	**5.5 (T)**	−1.1	**−4.3 (AT)**	
IP3: {Node 0 ⇒ 2 ⇒ end node 6}	n	6	4	41	51
	e	17.3	11.1	22.6	51
	z	**−4.5 (AT)**	**−3.2 (AT)**	**6.9 (T)**	
IP4: {Node 0 ⇒ 2 ⇒ 5 ⇒ end node 7}	n	8	0	2	10
	e	3.4	2.2	4.4	10
	z	**3.2 (T)**	−1.7	−1.6	
IP5: {Node 0 ⇒ 2 ⇒ 5 ⇒ end node 8}	n	4	13	6	23
	e	7.8	5.0	10.2	23
	z	−1.9	**4.5 (T)**	−2.0	
Total	n	39	25	51	115

Note: Global test results: $CHI^2 = 86.31$, df = 8, $p = 0.000$; Cramér's V = 0.613. Shown here are observed counts (n), expected counts (e) for the hypothesis of total independence, and adjusted residuals (z) to determine typical/overfrequented (T) and atypical/underfrequented (AT) cells. Bonferroni-adjusted level of significance: z {* = α/frequency of cells = 0.05/(5 × 3) = 0.00333} = 2.94. The bold values are statistically significant adjusted residuals.

3.3. Nitrous oxide (N_2O) emissions

The N_2O base sample tree selected six different variables (season & land-use, total phosphorus, carbon: nitrogen ratio, nitrate-nitrogen, total nitrogen, carbon: nitrogen ratio), thereby revealing seven effects that explained the emission rate variation in the study area. These effects were characterized by up to five-fold interactions (Fig. 4). Interestingly, the N_2O tree was the only tree of the three GHGs that exhibited an uneven split of the profile variable. As shown by the first pathway (IP1: node 0 ⇒ end node 1), the farmland during the dry season featured almost entirely high emission cases. However, this was a solitaire effect as no further interaction effects could be detected.

All other pathways led through the three remaining profile variable cases (i.e., wetland during the dry season and both land-use types during the rainy season) in the first step down the decision tree. Three interaction pathways showed a dominance of medium emission cases: IP2 (node 0 ⇒ 2 ⇒ 3 ⇒ end node 5) suggested that medium emission rates were supported by total phosphorus ≤40 ppm and carbon: nitrogen ratio ≤ 10. Interaction effect pathway three (IP3: node 0 ⇒ 2 ⇒ 3 ⇒ end node 6) indicated that high emissions were supported by total phosphorus ≤40 ppm and carbon: nitrogen ratio > 10. If total phosphorus exceeded 40 ppm and nitrate-nitrogen >0.2 g kg^{-1}, medium emissions dominated (IP4: node 0 ⇒ 2 ⇒ 4 ⇒ end node 8). Or, if total phosphorus was high, but nitrate-nitrogen low, total nitrogen ≤0.3% could also promote medium emissions (IP5: node 0 ⇒ 2 ⇒ 4 ⇒ 7 ⇒ end node 9). Pathways six and seven showed five-fold interactions of the following parameters: profile variable {season & land-use}, total phosphorus, nitrate-nitrogen, total nitrogen concentration, carbon: nitrogen ratio. Regarding the last split, a low carbon: nitrogen ratio (≤10) favored low emissions (IP6: node 0 ⇒ 2 ⇒ 4 ⇒ 7 ⇒ 10 ⇒ end node 11), whereas a higher ratio favored both low and medium emissions (IP7: node 0 ⇒ 2 ⇒ 4 ⇒ 7 ⇒ 10 ⇒ end node 12) (Fig. 4).

Overall, the N_2O tree showed a correct classification rate of more than two-thirds. All three emission groups performed equally well in classifying the effects (Table 7).

As shown in Table 8, only five of 21 cells exhibited a high hit probability. These distinctive features were found in four of seven pathways. The high emissions group was particularly prevalent in the farmland during the dry season (IP1). In the wetland during the dry season and in both land-use types during the rainy season, emissions were likely to be moderate if total phosphorus remained below 40 ppm and carbon: nitrogen ratio below 10 (IP2), albeit this effect was only slightly above the significance threshold. In contrast, when the carbon: nitrogen ratio exceeds 10, the high emissions group becomes prevalent (IP3). Also, at a low carbon: nitrogen ratio, the emissions were distinguished by a predominance of lower cases and a lack of the medium emissions group (IP6).

4. Discussion

4.1. CH_4 emissions

In the Anyiko wetland, there were CH_4 emissions and uptake, whereas, in the farmland, there was an uptake. Season did not influence the emission rates. The CH_4 emissions from the wetland were driven by the high soil organic carbon content (>3%) and high soil moisture (>90%). According to Reddy and DeLaune (2008), water-saturated conditions in wetland soil minimizes oxygen supply, thereby resulting in anaerobic decomposition of soil organic carbon and, consequently, the production of CH_4. Also, soil organic carbon supply is the main driver for methanogenesis once anaerobic conditions have established (Whalen, 2005). Methanogenic bacteria use soil organic carbon as a

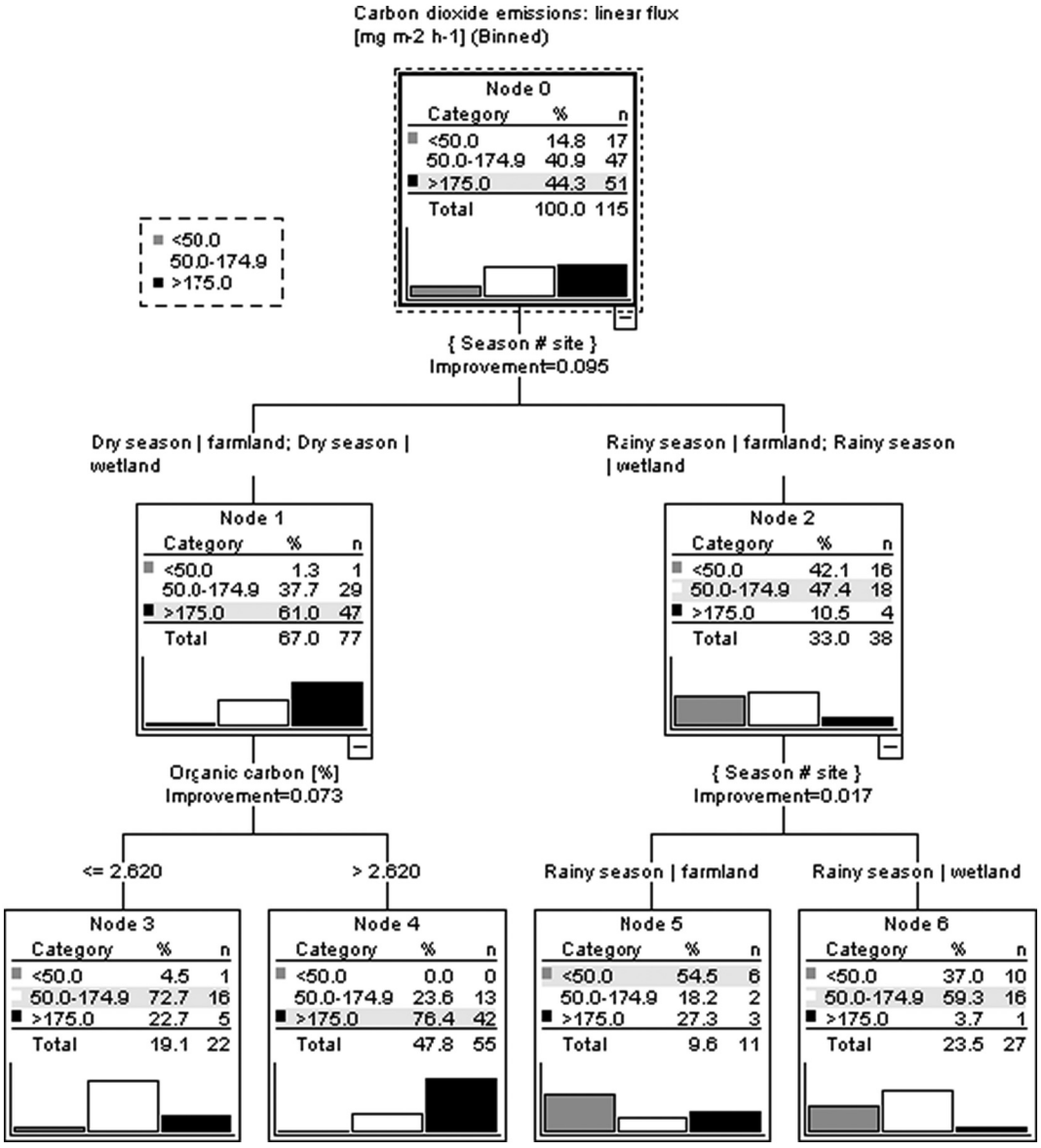

Fig. 3. Explorative decision tree (CRT) of the effects of land-use & season and soil parameters on CO_2 emissions. Minimum numbers of cases per parent node: 12; per child node: 8.

substrate during methanogenesis, and hence its availability enhances CH_4 emissions (Segers, 1998; Torres-Alvarado et al., 2005). The CH_4 uptake in the wetland, in contrast, was attributed to the low soil moisture ≤90%. This is anticipated because soil moisture is low under water-unsaturated conditions; therefore, the aerobic surface layers of wetlands can serve as CH_4 sinks (Horz et al., 2002; Reddy and DeLaune, 2008).

The drainage of wetlands increases the oxygen diffusion and reduces soil moisture content, ensuring aerobic conditions supporting methanotrophs, which leads to CH_4 uptake (Reddy and DeLaune, 2008; Smith et al., 2003). This pattern could be observed in the farmland (Fig. 2). Unlike the wetland, the farmland's CH_4 sink function was attributed to high soil NO_3-N concentrations. This observation's likely cause is that aerobic conditions in the farmland enhance the nitrification process, thereby resulting in increased NO_3-N concentrations in the soil, which is used to oxidize CH_4 by methanotrophs (van Grinsven et al., 2020).

Considering that the Anyiko wetland is seasonally inundated, it is expected that flooding during the rainy season would enhance CH_4 emissions, resulting in seasonal variations due to anaerobic conditions (Dalal et al., 2008; Liu et al., 2011). However, in the Anyiko wetland, flooding in LS1 was minimal due to water drainage measures. Hence, water mostly remained near the soil surface during the rainy season. Therefore, CH_4 produced in the oxygen-depleted soil zone may have been oxidized at the soil-water interface or the topsoil to CO_2 by methanotrophic bacteria, thereby reducing the CH_4 emissions (Lai, 2009).

Consistent with our findings, Were et al. (2021) reported no significant seasonal variations in CH_4 emissions in a wetland in Uganda.

Table 5
Classification table (observed versus predicted) of the CO_2 emissions tree (see Fig. 3).

Observed	Predicted			Percent correct
	1: <50.0	2: 50.0–174.99	3: ≥175.0	
1: <50.0	6	11	0	35.3%
2: 50.0–174.99	2	32	13	68.1%
3: ≥175.0	3	6	42	82.4%
Overall percentage	9.6%	42.6%	47.8%	69.6%

Table 6
Cross-classification table (CFA) results for the end nodes (interaction pathways) versus CO_2 emission groups (see Fig. 3).

Interaction pathway (IP) → end node		CO_2 emissions [mgm^{-2} h^{-1}]: classified			Total
		1: <50.0	2: 50.0–174.99	3: ≥175.0	
IP1: {Node 0 ⇒ 1 ⇒ end node 3}	n	1	16	5	22
	e	3.3	9.0	9.8	22
	z	−1.5	**3.4 (T)**	−2.3	
IP2: {Node 0 ⇒ 1 ⇒ end node 4}	n	0	13	42	55
	e	8.1	22.5	24.4	55
	z	**−4.3 (AT)**	**−3.6 (AT)**	**6.6 (T)**	
IP3: {Node 0 ⇒ 2 ⇒ end node 5}	n	6	2	3	11
	e	1.6	4.5	4.9	11
	z	**3.9 (T)**	−1.6	−1.2	
IP4: {Node 0 ⇒ 2 ⇒ end node 6}	n	10	16	1	27
	e	4.0	11.0	12.0	27
	z	**3.7 (T)**	2.2	**−4.9 (AT)**	
Total	n	17	47	51	115

Note: Global test results: $CHI^2 = 69.39$, df = 6 p = 0.000; Cramér's V = 0.549. Shown here are observed counts (n), expected counts (e) for the hypothesis of total independence, and adjusted residuals (z) to determine typical/over frequented (T) and atypical/under frequented (AT) cells. Bonferroni-adjusted level of significance: z {* = α/frequency of cells = 0.05/(4 × 3) = 0.00416} = 2.87. The bold values are statistically significant adjusted residuals.

However, Marín-Muñiz et al. (2015) reported higher CH_4 emissions during the rainy season (992.1 ± 313 mg m^{-2} d^{-1}) than during the dry season (160.8 ± 104 mg m^{-2} d^{-1}) in tropical freshwater marshes on the coastal plain of Veracruz in Mexico. During the rainy season, higher emissions were attributed to the higher water depths, increasing reduced soil conditions. Marín-Muñiz et al. (2015) reported the highest CH_4 emissions when the water depth was only 10 cm deep above the soil surface. In contrast, Mitsch et al. (2010) and Nahlik and Mitsch (2011) reported the highest CH_4 emissions when the water depths were 15–30 cm and 30–50 cm above the soil surface, respectively. An increase of the water column beyond these depths creates a CH_4 oxidation zone by methanotrophs that can mitigate CH_4 diffusion to the atmosphere (Nahlik and Mitsch, 2011). In contrast, Brown et al. (2014) reported the highest CH_4 emissions when the water depth dropped to 40 to 55 cm below the soil surface. They attributed the highest emissions to the establishment of required redox potentials and available substrates for methanogenesis. The reduction in water depth can also enhance CH_4 emissions due to an increase in the CH_4 diffusivity in the unsaturated zone (Brown et al., 2014). However, Moore et al. (2011) and Yan et al. (2020) reported positive linear relationships between the water depth and CH_4 emissions. A low water table in these studies was associated with more oxidizing conditions causing the reduction in CH_4 emissions. The use of carbon isotopic signatures ($\delta^{13}C$) such as done by Marushchak et al. (2016), Münchberger et al. (2019), and Popp et al. (1999) can aid in the identification of mechanisms and pathways of CH_4 dynamics with changing water depth. Therefore, future studies should consider stable isotope analyses along with the CH_4 flux measurements.

4.2. CO_2 emissions

The drainage of wetlands creates aerobic conditions that accelerate soil organic carbon decomposition, consequently increasing CO_2 emissions (Hirano et al., 2012; Mitsch et al., 2013; Syvitski et al., 2009). In our study, CO_2 emissions from the wetland and the farmland were not significantly different. Similar findings were reported by Inubushi et al. (2003). Medium to high CO_2 emissions (>50 mg m^{-2} d^{-1}) during the dry season and low emissions (<50 mg m^{-2} d^{-1}) during the rainy season may be associated with more oxidized conditions during the dry season. According to Smith et al. (2003), oxic conditions enhance aerobic decomposition of soil organic carbon, thus increasing CO_2 emissions. Furthermore, high and moderate CO_2 emissions were attributed to soil organic carbon content. Organic matter available for aerobic decomposition increases with decreasing soil water table during the dry season (Jauhiainen et al., 2008). We did not measure the water table in our study sites. However, from our observation during the rainy season, the water depths were well above the soil surface

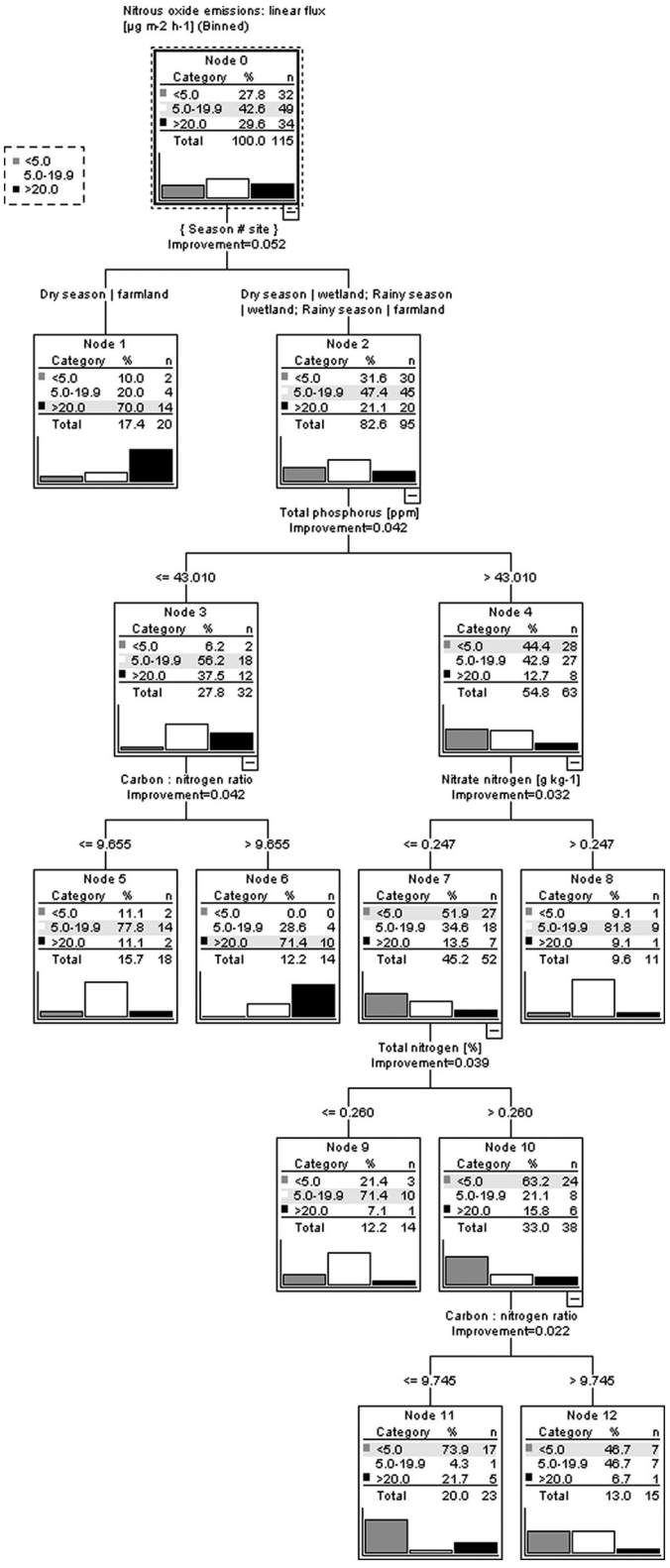

Fig. 4. Explorative decision tree (CRT) of the effects of land-use & season and soil parameters on N_2O emissions. Minimum numbers of cases per parent node: 12; per child node: 8.

Table 7
Classification table (observed versus predicted) of the N_2O emissions tree (see Fig. 4).

Observed	Predicted			Percent correct
	1: <5.0	2: 5.0–19.99	3: ≥20.0	
1: <5.0	24	6	2	75.0%
2: 5.0–19.99	8	33	8	67.3%
3: ≥20.0	6	4	24	70.6%
Overall percentage	33.0%	37.4%	29.6%	70.4%

(approximately 15 cm) in US2 and near the soil surface in LS1 and some parts of the farmland. Therefore, this water-logged situation in the rainy season could have contributed to the observed low CO_2 emissions from both land-use types. During the dry season, the study sites' water levels were below the soil surface and therefore expected to enhance oxidized conditions, reduce CH_4 emissions, and increase CO_2 emissions. Therefore, an increase in CO_2 emissions during the dry season can partly be ascribed to reduced methanogenesis and the considerable potential for microbial CH_4 oxidation in the oxygenated soil layer (Preuss et al., 2013; Segers, 1998).

Our findings are consistent with Jun-Qin et al. (2009), who reported an increase in CO_2 emissions with declining water saturation in a laboratory incubation experiment of Zoige Alpine wetland soils in China. Were et al. (2021) though reported higher CO_2 emissions than our findings, they also had higher emissions during the dry than rainy seasons. Similarly, Marín-Muñiz et al. (2015) also reported findings with higher mean CO_2 emissions during the dry season (11.7 ± 1.1 g m^{-2} d^{-1}) than during the rainy season (4.2 ± 0.52 g m^{-2} d^{-1}).

4.3. N_2O emissions

High N_2O emissions from the farmland during the dry season may be attributed to the farmland's enhanced nitrification processes. The drainage of wetlands coupled with low soil moisture during the dry season enhances the soil's oxic conditions, increasing mineralization of organic nitrogen and subsequent nitrification processes (Jauhiainen et al., 2012; Venterink et al., 2002). Under low oxygen conditions, nitrifiers reduce nitrite (NO_2-N) produced during the nitrification process to N_2O (Reddy and DeLaune, 2008; Signor and Cerri, 2013). According to van Lent et al. (2015), higher N_2O emissions from the farmland would occur in the first ten years after conversion and decline if the farmland remains unfertilized. Also, Owino et al. (2020) reported higher N_2O emissions from fertilized (4.4 ± 3.2 μg m^{-2} h^{-1}) than unfertilized (-3.6 ± 2.6 μg m^{-2} h^{-1}) paddy rice fields converted for the last four decades from the Anyiko wetland in Kenya. The conversion decreases soil organic carbon and nitrogen, which are substrates for the nitrification and denitrification processes (Cameron et al., 2013). In our study, the farmland was established 1–2 years before the GHG sampling. Also, usage of other sources of nitrogen such as livestock manure in the farmland is unlikely as each farmer owns around three cattle (range: 1–8 cattle), and livestock manure is mainly used in the infertile upland farms (Ondiek et al., unpublished data). Therefore, in SSA, higher N_2O emissions from farmland, particularly during the dry season, are possibly linked to the number of years the converted areas have been cultivated, even though there are non-intensive agricultural practices. However, this phenomenon warrants further studies. These studies should also extend GHG sampling for a minimum of one year to increase the accuracy of cumulative seasonal GHG emissions (see Butterbach-Bahl et al., 2016).

Furthermore, our results showed that, regardless of the season, N_2O emissions from the wetland and the farmland during the rainy season were quite diverse. If total phosphorous was below 40 ppm and carbon: nitrogen ratio > 10 in sediments, higher emissions were observed, whereas a lower carbon: nitrogen (≤10) ratio supported moderate emissions. Carbon: nitrogen ratios less than 30 support net nitrogen mineralization and associated nitrification, increasing the availability of NH_4-N and NO_3-N, which are substrates for coupled nitrification-denitrification processes (Butterbach-Bahl et al., 2013). Therefore, in this study, net nitrogen mineralization and subsequent substrates were enhanced when C: N ratios were >10 and reduced when the ratios were ≤10. The low N_2O emissions were possibly linked to reduced nitrification process since soil NO_3-N content were low. Under more anaerobic conditions than aerobic, nitrification process is reduced (Jiang et al., 2009; Reddy and DeLaune, 2008). N_2O emissions through the denitrification process may decline due to low concentrations of NO_3-N (Page and Dalal, 2011). Also, under strict anaerobic conditions, the major end-product of denitrification is N_2 (Butterbach-Bahl et al., 2013), thus explaining the very low N_2O emissions from the wetland in both seasons and from the farmland during the rainy season. Our study did not investigate seasonal changes in the emissions of N_2O: N_2 ratios and therefore needs further research to quantify this aspect.

Table 8
Cross-classification table (CFA) results for the end nodes (interaction pathways) versus N_2O emission groups (see Fig. 4).

Interaction pathway (IP) → end node		N_2O emissions [μgm^{-2} h^{-1}]: classified			Total
		1: < 5.0	2: 5.0–19.99	3: ≥20.0	
IP1: {Node 0 ⇒ end node 1}	n	2	4	14	20
	e	5.6	8.5	5.9	20
	z	−2.0	−2.2	**4.4 (T)**	
IP2: {Node 0 ⇒ 2 ⇒ 3 ⇒ end node 5}	n	2	14	2	18
	e	5.0	7.7	5.3	18
	z	−1.7	**3.3 (T)**	−1.9	
IP3: {Node 0 ⇒ 2 ⇒ 3 ⇒ end node 6}	n	0	4	10	14
	e	3.9	6.0	4.1	14.0
	z	−2.5	−1.1	**3.7 (T)**	
IP4: {Node 0 ⇒ 2 ⇒ 4 ⇒ end node 8}	n	1	9	1	11
	e	3.1	4.7	3.3	11
	z	−1.5	2.8	−1.6	
IP5: {Node 0 ⇒ 2 ⇒ 4 ⇒ 7 ⇒ end node 9}	n	3	10	1	14
	e	3.9	6.0	4.1	14
	z	−0.6	2.3	−2	
IP6: {Node 0 ⇒ 2 ⇒ 4 ⇒ 7 ⇒ 10 ⇒ end node 11}	n	17	1	5	23
	e	6.4	9.8	6.8	23
	z	**5.5 (T)**	**−4.1 (AT)**	−0.9	
IP7: {Node 0 ⇒ 2 ⇒ 4 ⇒ 7 ⇒ 10 ⇒ end node 12}	n	7	7	1	15
	e	4.2	6.4	4.4	15
	z	1.7	0.3	−2.1	
Total	n	32	49	34	115

Note: Global test results: $CHI^2 = 80.49$, df = 12, $p = 0.000$; Cramér's V = 0.592. Shown here are observed counts (n), expected counts (e) for the hypothesis of total independence, and adjusted residuals (z) to determine typical/over frequented (T) and atypical/under frequented (AT) cells. Bonferroni-adjusted level of significance: z {* = α/frequency of cells = 0.05/(7 × 3) = 0.00238} = 3.04. The bold values are statistically significant adjusted residuals.

4.4. Bootstrapping validation

Considering that the dataset did not fulfill an experiment's requirements from a statistical point of view, we had to interpret the results presented herein from a hypothesis-generating perspective. Nevertheless, it would be possible to further evaluate the stability of the detected effects to validate the results, thereby strengthening the notion that results can be generalized. To achieve this, the classical bootstrapping approach may be used to re-sample the base sample and re-run the decision trees. However, to also detect additional effects and longer interaction chains, a modified variant of the bootstrapping method, cumulative/pooled bootstrapping (Hayes et al., 2021), provides a more viable procedure.

Re-running the tree analyses with an inflated dataset through cumulative bootstrapping shows that the splits related to land-use and season remain stable, confirming the influence of this controlling effect. In the case of all three GHGs, the decision trees of the cumulative

bootstrapping dataset split the tree into broader and deeper levels, allowing the identification of more interaction effect pathways than the base sample versions. While the base sample trees of CH_4, CO_2, and N_2O selected four, two, and five parameters, respectively, the trees of the cumulative bootstrap samples chose five, six, and five parameters, respectively. Hence, the bootstrapped trees extended the list of parameters already detected in the base sample trees.

Overall, the cumulative bootstrapping simulation exhibits an increased performance capability compared to the standard version. Hence, the modified variant deserves a more detailed demonstration and a more prominent and broader methodological discussion. In our opinion, this can and should be realized in a follow-up paper.

5. Conclusion

The conversion of the Anyiko wetland areas to farmland resulted in larger CH_4 uptakes irrespective of season, and high N_2O emissions during the dry season. Although CO_2 emissions were not influenced by land-use, season was a primary influence, as higher emissions were observed in the dry than in the rainy season. The CH_4 uptake and higher CO_2 emissions were related to soil NO_3-N and organic carbon content, respectively. The high N_2O outputs in the farmland during the dry season was a solitaire effect as no further interaction effects could be detected. In light of hypothesis-exploration approaches, our findings should be subject to follow-up studies. In this regard, it is recommended to conduct sampling for at least one year. Such an approach would increase the accuracy of cumulative seasonal and annual GHG emissions as well as provide a larger sample size, therefore possibly indicating which soil properties potentially drive the emissions.

Funding

We are thankful to the Austrian Development Corporation (ADC) and the Austrian Partnership Programme in Higher Education and Research for Development (APPEAR), a programme of the Austrian Development Cooperation (ADC) and implemented by Austria's Agency for Education and Internationalisation (OeAD) for funding this study.

CRediT authorship contribution statement

Risper Ajwang' Ondiek: Conceptualization, Methodology, Investigation, Data curation, Writing – original draft, Writing – review & editing. **Daniel S. Hayes:** Formal analysis, Data curation, Writing – original draft, Writing – review & editing. **Damaris Njeri Kinyua:** Conceptualization, Methodology, Investigation, Writing – review & editing. **Nzula Kitaka:** Conceptualization, Methodology, Writing – review & editing. **Erwin Lautsch:** Formal analysis, Data curation, Writing – review & editing. **Paul Mutuo:** Methodology, Data curation, Writing – review & editing. **Thomas Hein:** Conceptualization, Methodology, Data curation, Writing – review & editing.

Declaration of competing interest

The authors declare that they have no known competing financial interests or personal relationships that could have appeared to influence the work reported in this paper.

Acknowledgements

We are grateful for the support of the Limnology and Wetland Management Programme (LWM) at Egerton University in Kenya, International Training Programmes in Limnology (IPGL) at the University of Natural Resources and Life Sciences in Vienna, and Doctoral School Human River Systems in the 21st Century (HR21) at the University of Natural Resources and Life Sciences in Vienna. We appreciate the support from the Forest Research Center, a research unit funded by Fundação para a Ciência e a Tecnologia I.P. (FCT), Portugal (UID/AGR/00239/2013).

Appendix A. Supplementary data

Supplementary data to this article can be found online at https://doi.org/10.1016/j.scitotenv.2021.147701.

References

Altieri, M. A., & Koohafkan, P. (2008). Enduring farms: climate change, smallholders and traditional farming communities: Third World Network (TWN) Penang (Vol. 6).

Arias-Navarro, C., Díaz-Pinés, E., Kiese, R., Rosenstock, T.S., Rufino, M.C., Stern, D., ... Butterbach-Bahl, K., 2013. Gas pooling: a sampling technique to overcome spatial heterogeneity of soil carbon dioxide and nitrous oxide fluxes. Soil Biol. Biochem. 67, 20–23.

Batson, J., Noe, G.B., Hupp, C.R., Krauss, K.W., Rybicki, N.B., Schenk, E.R., 2015. Soil greenhouse gas emissions and carbon budgeting in a short-hydroperiod floodplain wetland. J. Geophys. Res. Biogeosci. 120, 77–95.

Bergamaschi, P., Frankenberg, C., Meirink, J., Krol, M., Dentener, F., Wagner, T., Heimann, M., 2007. Satellite chartography of atmospheric methane from SCIAMACHY on board ENVISAT: 2. Evaluation based on inverse model simulations. J. Geophys. Res. Atmos. 112, D02304–….

Bernal, B., Mitsch, W.J., 2012. Comparing carbon sequestration in temperate freshwater wetland communities. Glob. Chang. Biol. 18, 1636–1647.

Bernal, B., Mitsch, W.J., 2013. Carbon sequestration in freshwater wetlands in Costa Rica and Botswana. Biogeochemistry 115, 77–93.

Bloom, A.A., Palmer, P.I., Fraser, A., Reay, D.S., Frankenberg, C., 2010. Large-scale controls of methanogenesis inferred from methane and gravity spaceborne data. Science 327, 322–325.

Breiman, L., Friedman, J.H., Olshen, R.A., Stone, C.J., 1984. Classification and Regression Trees. Chapman & Hall/CRC, New York.

Bridgham, S.D., Megonigal, J.P., Keller, J.K., Bliss, N.B., Trettin, C., 2006. The carbon balance of North American wetlands. Wetlands 26, 889–916.

Brown, M.G., Humphreys, E.R., Moore, T.R., Roulet, N.T., Lafleur, P.M., 2014. Evidence for a nonmonotonic relationship between ecosystem-scale peatland methane emissions and water table depth. J. Geophys. Res. Biogeosci. 119, 826–835.

Butterbach-Bahl, K., Kiese, R., Liu, C., 2011. Measurements of biosphere–atmosphere exchange of CH_4 in terrestrial ecosystems. Methods in Enzymology. Vol. 495. Elsevier, pp. 271–287.

Butterbach-Bahl, K., Baggs, E.M., Dannenmann, M., Kiese, R., Zechmeister-Boltenstern, S., 2013. Nitrous oxide emissions from soils: how well do we understand the processes and their controls? Philos. Trans. R. Soc. B Biol. Sci. 368, 20130122.

Butterbach-Bahl, K., Sander, B.O., Pelster, D., Díaz-Pinés, E., 2016. Quantifying greenhouse gas emissions from managed and natural soils. Methods for Measuring Greenhouse Gas Balances and Evaluating Mitigation Options in Smallholder Agriculture. Springer, Cham, pp. 71–96.

Cameron, K., Di, H.J., Moir, J., 2013. Nitrogen losses from the soil/plant system: a review. Ann. Appl. Biol. 162, 145–173.

County Government of Siaya, 2018. County Integrated Development Plan 2018–2022.

Croghan, C., Egeghy, P.P., 2003. Methods of dealing with values below the limit of detection using SAS. South. SAS User Group 22, 24.

Dalal, R., Allen, D., Livesley, S., Richards, G., 2008. Magnitude and biophysical regulators of methane emission and consumption in the Australian agricultural, forest, and submerged landscapes: a review. Plant Soil 309, 43–76.

Davidson, E.A., Janssens, I.A., 2006. Temperature sensitivity of soil carbon decomposition and feedbacks to climate change. Nature 440, 165–173.

Dixon, A.B., Wood, A.P., 2003. Wetland cultivation and hydrological management in eastern Africa: matching community and hydrological needs through sustainable wetland use. Paper Presented at the Natural Resources Forum.

Euliss, N.H., Gleason, R., Olness, A., McDougal, R., Murkin, H., ... Robarts, R.Warner, 2006. North American prairie wetlands are important nonforested land-based carbon storage sites. Sci. Total Environ. 361, 179–188.

van Grinsven, S., Sinninghe Damsté, J.S., Harrison, J., Polerecky, L., Villanueva, L., 2020. Nitrate promotes the transfer of methane-derived carbon from the methanotroph Methylobacter sp. to the methylotroph Methylotenera sp. in eutrophic lake water. Limnology and Oceanography.

Hayes, D.S., Brändle, J.M., Seliger, C., Zeiringer, B., Ferreira, T., Schmutz, S., 2018. Advancing towards functional environmental flows for temperate floodplain rivers. Sci. Total Environ. 633, 1089–1104.

Hayes, D.S., Lautsch, E., Unfer, G., Greimel, F., Zeiringer, B., Höller, N., Schmutz, S., 2021. Response of European grayling, Thymallus thymallus, to multiple stressors in hydropeaking rivers. J. Environ. Manag. 292, 112737.

Hernandez, M.E., Mitsch, W.J., 2007. Denitrification in created riverine wetlands: influence of hydrology and season. Ecol. Eng. 30, 78–88.

Hirano, T., Segah, H., Kusin, K., Limin, S., Takahashi, H., Osaki, M., 2012. Effects of disturbances on the carbon balance of tropical peat swamp forests. Glob. Chang. Biol. 18, 3410–3422.

Horz, H.P., Raghubanshi, A.S., Heyer, J., Kammann, C., Conrad, R., Dunfield, P.F., 2002. Activity and community structure of methane-oxidising bacteria in a wet meadow soil. FEMS Microbiol. Ecol. 41, 247–257.

Houghton, R.A., House, J., Pongratz, J., Van Der Werf, G., DeFries, R., Hansen, M., ... Ramankutty, N., 2012. Carbon emissions from land use and land-cover change. Biogeosciences 5125–5142.
IBM Statistics, 2016. IBM SPSS Statistics 24 Algorithms.
Inubushi, K., Furukawa, Y., Hadi, A., Purnomo, E., Tsuruta, H., 2003. Seasonal changes of CO_2, CH_4 and N_2O fluxes in relation to land-use change in tropical peatlands located in coastal area of South Kalimantan. Chemosphere 52, 603–608.
IPCC, 2013. Climate Change 2013: The Physical Science Basis. Contribution of Working Group I to the Fifth Assessment Report of the Intergovernmental Panel on Climate Change. Cambridge, United Kingdom and New York, NY, USA.
Jauhiainen, J., Limin, S., Silvennoinen, H., Vasander, H., 2008. Carbon dioxide and methane fluxes in drained tropical peat before and after hydrological restoration. Ecology 89, 3503–3514.
Jauhiainen, J., Silvennoinen, H., Hämäläinen, R., Kusin, K., Limin, S., Raison, R., Vasander, H., 2012. Nitrous oxide fluxes from tropical peat with different disturbance history and management. Biogeosciences 9, 1337.
Jiang, C., Wang, Y., Hao, Q., Song, C., 2009. Effect of land-use change on CH_4 and N_2O emissions from freshwater marsh in Northeast China. Atmos. Environ. 43, 3305–3309.
Junk, W.J., An, S., Finlayson, C., Gopal, B., Květ, J., Mitchell, S.A., ... Robarts, R.D., 2013. Current state of knowledge regarding the world's wetlands and their future under global climate change: a synthesis. Aquat. Sci. 75, 151–167.
Jun-Qin, G., Ouyang, H., Xing-Liang, X., Cai-Ping, Z., Zhang, F., 2009. Effects of temperature and water saturation on CO_2 production and nitrogen mineralization in alpine wetland soils. Pedosphere 19, 71–77.
Lai, D., 2009. Methane dynamics in northern peatlands: a review. Pedosphere 19, 409–421.
van Lent, J., Hergoualc'h, K., Verchot, L., 2015. Reviews and syntheses: soil N_2O and NO emissions from land use and land-use change in the tropics and subtropics: a meta-analysis. Biogeosciences 12, 7299–7313.
Lienert, G.A., 1978. Verteilungsfreie Methoden in der Biostatistik. Verlag Anton Hain, Meisenheim am Glan.
Liu, D., Ding, W., Jia, Z., Cai, Z., 2011. Relation between methanogenic archaea and methane production potential in selected natural wetland ecosystems across China. Biogeosciences 8, 329.
Liu, X., Jiang, M., Dong, G., Zhang, Z., Wang, X., 2017. Ecosystem service comparison before and after marshland conversion to paddy field in the Sanjiang Plain, Northeast China. Wetlands 37, 593–600.
Marín-Muñiz, J.L., Hernández, M.E., Moreno-Casasola, P., 2015. Greenhouse gas emissions from coastal freshwater wetlands in Veracruz Mexico: effect of plant community and seasonal dynamics. Atmos. Environ. 107, 107–117.
Marushchak, M., Friborg, T., Biasi, C., Herbst, M., Johansson, T., Kiepe, I., ... Virtanen, T., 2016. Methane dynamics in the subarctic tundra: combining stable isotope analyses, plot-and ecosystem-scale flux measurements. Biogeosciences 13, 597–608.
MEA, 2005. Ecosystems and Human Well-Being Wetlands and Water Synthesis. World Resources Institute, Washington, DC.
MEMR, 2012. Kenya Wetlands Atlas. Ministry of Environment and Mineral Resources, Nairobi.
Minamikawa, K., Yagi, K., Tokida, T., Sander, B.O., Wassmann, R., 2012. Appropriate frequency and time of day to measure methane emissions from an irrigated rice paddy in Japan using the manual closed chamber method. Greenhouse Gas Measure. Manage. 2, 118–128.
Mitchell, S.A., 2013. The status of wetlands, threats and the predicted effect of global climate change: the situation in Sub-Saharan Africa. Aquat. Sci. 75, 95–112.
Mitsch, W., Gosselink, J., 2007. Wetlands. 4th ed. Wiley, Hoboken.
Mitsch, W.J., Nahlik, A., Wolski, P., Bernal, B., Zhang, L., Ramberg, L., 2010. Tropical wetlands: seasonal hydrologic pulsing, carbon sequestration, and methane emissions. Wetl. Ecol. Manag. 18, 573–586.
Mitsch, W.J., Bernal, B., Nahlik, A.M., Mander, Ü., Zhang, L., Anderson, C.J., ... Brix, H., 2013. Wetlands, carbon, and climate change. Landsc. Ecol. 28, 583–597.
Moore, T.R., De Young, A., Bubier, J.L., Humphreys, E.R., Lafleur, P.M., Roulet, N.T., 2011. A multi-year record of methane flux at the Mer Bleue bog, southern Canada. Ecosystems 14, 646–657.
Münchberger, W., Knorr, K.-H., Blodau, C., Pancotto, V.A., Kleinebecker, T., 2019. Zero to moderate methane emissions in a densely rooted, pristine Patagonian bog—biogeochemical controls as revealed from isotopic evidence. Biogeosciences 16, 541–559.
Nahlik, A.M., Mitsch, W.J., 2011. Methane emissions from tropical freshwater wetlands located in different climatic zones of Costa Rica. Glob. Chang. Biol. 17, 1321–1334.
Nath, A.J., Lal, R., 2017. Managing tropical wetlands for advancing global rice production: implications for land-use management. Land Use Policy 68, 681–685.
Okalebo, J.R., Gathua, K.W., Woomer, P.L., 2002. Laboratory Methods of Soil and Plant Analysis: A Working Manual. Second edition. Sacred Africa, Nairobi.
Ondiek, R., Vuolo, F., Kipkemboi, J., Kitaka, N., Lautsch, E., Hein, T., Schmid, E., 2020. Socio-economic determinants of land use/cover change in wetlands in East Africa: a case study analysis of the Anyiko wetland, Kenya. Front. Environ. Sci. 7, 207.
Owino, A.O., Ryan, P.G., 2007. Recent papyrus swamp habitat loss and conservation implications in western Kenya. Wetl. Ecol. Manag. 15, 1–12.
Owino, C.N., Kitaka, N., Kipkemboi, J., Ondiek, R.A., 2020. Assessment of greenhouse gases emission in smallholder rice paddies converted from Anyiko Wetland, Kenya. Front. Environ. Sci. 8, 80.
Page, K., Dalal, R., 2011. Contribution of natural and drained wetland systems to carbon stocks, CO_2, N_2O, and CH_4 fluxes: an Australian perspective. Soil Res. 49, 377–388.
Parkin, T.B., Venterea, R.T., 2010. USDA-ARS GRACEnet Project Protocols, Chapter 3. Chamber-based Trace Gas Flux Measurements. Sampling Protocols. Beltsville, MD. pp. 1–39.
Parkin, T.B., Venterea, R.T., Hargreaves, S.K., 2012. Calculating the detection limits of chamber-based soil greenhouse gas flux measurements. J. Environ. Qual. 41, 705–715.
Pelster, D., Rufino, M.C., Rosenstock, T., Mango, J., Saiz, G., Diaz Pines, E., ... Butterbach Bahl, K., 2017. Smallholder Farms in Eastern African Tropical Highlands Have Low Soil Greenhouse Gas Fluxes.
Popp, T.J., Chanton, J.P., Whiting, G.J., Grant, N., 1999. Methane stable isotope distribution at a Carex dominated fen in north central Alberta. Glob. Biogeochem. Cycles 13, 1063–1077.
Preuss, I., Knoblauch, C., Gebert, J., Pfeiffer, E.-M., 2013. Improved quantification of microbial CH_4 oxidation efficiency in arctic wetland soils using carbon isotope fractionation. Biogeosciences 10.
Pumpanen, J., Kolari, P., Ilvesniemi, H., Minkkinen, K., Vesala, T., Niinistö, S., ... Pihlatie, M., 2004. Comparison of different chamber techniques for measuring soil CO_2 efflux. Agric. For. Meteorol. 123, 159–176.
Reddy, K.R., DeLaune, R.D., 2008. Biogeochemistry of Wetlands: Science and Applications. CRC Press.
Rochette, P., 2011. Towards a standard non-steady-state chamber methodology for measuring soil N_2O emissions. Anim. Feed Sci. Technol. 166, 141–146.
Rochette, P., Bertrand, N., 2003. Soil air sample storage and handling using polypropylene syringes and glass vials. Can. J. Soil Sci. 83, 631–637.
Rochette, P., Bertrand, N., 2008. Soil-surface gas emissions. In: Carter, M., Gregorich, E.G. (Eds.), Soil Sampling and Methods of Analysis. CRC Press, Boca Raton, FL, USA.
Saunders, M.J., Kansiime, F., Jones, M.B., 2012. Agricultural encroachment: implications for carbon sequestration in tropical African wetlands. Glob. Chang. Biol. 18, 1312–1321.
Segers, R., 1998. Methane production and methane consumption: a review of processes underlying wetland methane fluxes. Biogeochemistry 41, 23–51.
Signor, D., Cerri, C.E.P., 2013. Nitrous oxide emissions in agricultural soils: a review. Pesq. Agr. Trop. 43, 322–338.
Smith, K., Conen, F., 2004. Impacts of land management on fluxes of trace greenhouse gases. Soil Use Manag. 20, 255–263.
Smith, K., Ball, T., Conen, F., Dobbie, K., Massheder, J., Rey, A., 2003. Exchange of greenhouse gases between soil and atmosphere: interactions of soil physical factors and biological processes. Eur. J. Soil Sci. 54, 779–791.
Syvitski, J.P., Kettner, A.J., Overeem, I., Hutton, E.W., Hannon, M.T., Brakenridge, G.R., ... Giosan, L., 2009. Sinking deltas due to human activities. Nat. Geosci. 2, 681–686.
Tangen, B.A., Finocchiaro, R.G., Gleason, R.A., 2015. Effects of land use on greenhouse gas fluxes and soil properties of wetland catchments in the Prairie Pothole Region of North America. Sci. Total Environ. 533, 391–409.
Torres-Alvarado, R., Ramírez-Vives, F., Fernández, F.J., Barriga-Sosa, I., 2005. Methanogenesis and methane oxidation in wetlands. Implications in the global carbon cycle. Hidrobiológica 15, 327–349.
Tshering, K., 2012. Measuring ecosystem functions; denitrification enzyme assay in Mara wetland, Tanzania. Sherub Doenme 11, 45–53.
Tukey, J. W. (1977). Exploratory Data Analysis.
Tully, K.L., Abwanda, S., Thiong'o, M., Mutuo, P.M., Rosenstock, T.S., 2017. Nitrous oxide and methane fluxes from urine and dung deposited on Kenyan pastures. J. Environ. Qual. 46, 921–929.
Venterink, H.O., Davidsson, T., Kiehl, K., Leonardson, L., 2002. Impact of drying and re-wetting on N, P and K dynamics in a wetland soil. Plant Soil 243, 119–130.
Von Eye, A., 2002. Configural Frequency Analysis: Methods, Models, and Applications. Lawrence Erlbaum Associates, Inc., Mahwah, NJ.
Von Eye, A., Mair, P., Mun, E.Y., 2010. Advances in Configural Frequency Analysis. Guilford Press, New York.
Wall, K.D., Lienert, G.A., 1976. A test for point-symmetry in J-dimensional contingency cubes. Biom. J. 18, 259–264.
Were, D., Kansiime, F., Fetahi, T., Hein, T., 2021. Carbon dioxide and methane fluxes from various vegetation communities of a natural tropical freshwater wetland in different seasons. Environmental Processes, pp. 1–19.
Whalen, S., 2005. Biogeochemistry of methane exchange between natural wetlands and the atmosphere. Environ. Eng. Sci. 22, 73–94.
Whiting, G.J., Chanton, J.P., 2001. Greenhouse carbon balance of wetlands: methane emission versus carbon sequestration. Tellus B 53, 521–528.
Yan, L., Zhang, X., Wu, H., Kang, E., Li, Y., Wang, J., ... Kang, X., 2020. Disproportionate changes in the CH_4 emissions of six water table levels in an Alpine peatland. Atmosphere 11, 1165.
Zedler, J.B., Kercher, S., 2005. Wetland resources: status, trends, ecosystem services, and restorability. Annu. Rev. Environ. Resour. 30, 39–74.
Zhu, X., Burger, M., Doane, T.A., Horwath, W.R., 2013. Ammonia oxidation pathways and nitrifier denitrification are significant sources of N_2O and NO under low oxygen availability. Proc. Natl. Acad. Sci. 110, 6328–6333.